Computational Intelligence in Electrical Engineering
Vol. 17, No. 1, 2026
pp. 45-58
Research Paper

Distribution Network Reconfiguration in the Presence of Distributed Generation Considering Non-Adaptive Overcurrent Relay Re-Coordination

Rasoul Abdollahi, [1], Reza Mohammadi Chabanloo [2*]

[1] Department of Electrical Engineering, Shahid Beheshti University, Tehran, Iran
r_abdollahi@sbu.ac.ir
[2] Department of Electrical Engineering, Shahid Beheshti University, Tehran, Iran
re_mohammadi@sbu.ac.ir

Abstract :
Distribution network reconfiguration can reduce feeder losses, but topology changes also modify branch currents and fault-current paths, which may compromise overcurrent-relay coordination. This issue becomes more complex in photovoltaic (PV)-integrated distribution networks because operating conditions vary with both load and PV generation. This paper extends an offline non-adaptive relay re-coordination framework to PV-integrated distribution-network reconfiguration under multiple load and PV operating scenarios. A Genetic Algorithm is used to determine feasible radial network configurations, while a Linear Programming subproblem determines one universal set of relay Time Multiplier Settings (TMS) that remains unchanged across all selected configurations and scenarios. The formulation minimizes active power loss subject to voltage, branch-current, PV operating, relay pickup, and coordination-time constraints. The method is evaluated on the IEEE 33-bus and Sirjan 78-bus distribution systems and compared with fixed-setting and adaptive-protection approaches. The results show that the proposed offline strategy expands the feasible configuration space and achieves loss performance close to adaptive protection while maintaining the required coordination margin without online relay-setting changes. The main contribution is therefore the extension of universal non-adaptive relay re-coordination to PV-integrated reconfiguration under load and PV variability, rather than the introduction of a new optimization algorithm or protection principle.
Keywords: Distribution Network Reconfiguration, Overcurrent Relay Re-Coordination, Non-Adaptive Protection, Renewable source integration.

1. Introduction

The increasing penetration of photovoltaic (PV) systems in distribution networks presents both opportunities and challenges for system operators. While PV generation reduces dependency on fossil fuels and decreases losses, its intermittent nature

* Submission date:17, 05, 2026
Acceptance date: 20, 10, 2026
Corresponding author: Rasoul Abdollahi, Department of Electrical Engineering, Shahid Beheshti University, Tehran, Iran
This is an open access article under the CC BY-NC-ND/4.0/ License (https://creativecommons.org/licenses/by-nc-nd/4.0/).
https://doi.org/10.22108/isee.2026.148914.1786

and bidirectional power flow complicate network operation and protection coordination. Distribution network reconfiguration (DNR) is a well-established strategy for optimizing network performance by altering topology through switch operations to minimize losses, improve voltage profiles, and balance loads. However, traditional reconfiguration methods often overlook the critical impact of topology changes on protection system coordination.

Protection systems in distribution networks rely on coordinated operation of overcurrent relays, reclosers, and fuses to isolate faults while maintaining service to healthy sections. Network reconfiguration can significantly alter fault current levels and directions, potentially disrupting this coordination. Existing approaches to address this challenge fall into two categories: (1) non-adaptive methods that discard configurations violating fixed protection settings, severely limiting optimization potential; and (2) adaptive protection schemes that require costly telecommunication infrastructure for real-time setting adjustments.

The integration of PV systems further complicates this problem. PV generation affects both load flow patterns and fault current contributions, introducing additional variability that must be considered in both reconfiguration and protection coordination. Most existing research either focuses on reconfiguration with fixed protection settings or addresses protection coordination for static network topologies. Few studies have investigated the co-optimization of reconfiguration and protection settings in PV-integrated networks

Distribution network reconfiguration has been extensively studied since the seminal work of [1]. Early approaches focused on loss minimization using heuristic methods like branch exchange [2] and optimal flow pattern algorithms [3]. With increasing computational power, metaheuristic methods including Genetic Algorithms [4], Particle Swarm Optimization [5], and Harmony Search [6] have been succe

ssfully applied. Recent research has expanded reconfiguration objectives to include reliability improvement [7], voltage stability enhancement [8], and integration of distributed generation [9].

Protection coordination ensures selective fault isolation through proper time-current characteristic coordination between upstream and downstream devices. Traditional coordination methods assume fixed network topology [10]. Several studies have addressed coordination challenges in networks with distributed generation [11, 12], noting that DG injection can reduce fault currents and potentially cause protection blinding. Adaptive protection schemes [13, 14] have been proposed to adjust settings dynamically but require communication infrastructure and raise cybersecurity concerns.

Limited research has integrated protection constraints into reconfiguration problems. Reference [15] formulated protection constraints as penalty functions in reconfiguration optimization but used fixed protection settings. Reference [16] proposed an algorithm considering protective device coordination but limited switching actions to maintain coordination. Reference [17] introduced offline re-coordination of overcurrent relays to expand feasible configurations but did not consider distributed generation.

PV integration affects both steady-state operation and protection systems. Unlike conventional synchronous generation, inverter-based PV sources have limited fault current contribution [18], which can affect relay operation times. Several studies have analyzed protection challenges in PV-rich networks [19, 20], but few have integrated these considerations into reconfiguration optimization. The uncertainty of renewable generation adds another layer of complexity, requiring probabilistic or scenario-based approaches [21].

Table (1): Literature review summary

Ref	Reconfiguration	Protection	DG/PV	Uncertainty	Adaptive/Non-adaptive
[4], [5], [6]	✓	✗	Limited	✗	-
[10], [11], [12]	✗	✓	Some	✗	Both
[15]	✓	Fixed settings	✗	✗	Non-adaptive
[16]	Limited	✓	✗	✗	Non-adaptive
[17]	✓	Re-coordination	✗	✗	Non-adaptive
[19], [20]	✗	✓	✓	Limited	Both
[21]	✓	Fixed settings	✓	✓	Non-adaptive
This paper	✓	Re-coordination	✓ (PV)	✓ (Scenario-based)	Non-adaptive

The distinction among [17], [21], and the present work is central to the contribution of this study. Reference [17] introduced offline non-adaptive overcurrent-relay re-coordination with one common relay-setting set across multiple reconfigured operating states, but did not consider distributed generation or PV uncertainty. Reference [21] considered distribution-network reconfiguration in the presence of distributed generation, protection constraints, and uncertainty; however, the protective-device settings were treated as fixed constraints rather than jointly re-coordinated as decision variables. The present work combines these two directions by extending offline universal relay re-coordination to PV-integrated operation under load and PV variability, while maintaining a single fixed TMS set across the selected configurations and operating scenarios.

As shown in Table 1, previous studies have separately addressed protection-aware reconfiguration, distributed-generation uncertainty, and non-adaptive relay re-coordination. However, the specific combination considered in this paper—PV/load operating uncertainty together with a single universal relay-setting set that remains valid across the selected reconfigured operating states—has not been explicitly addressed in the reviewed studies.

This paper fills this gap by proposing an offline optimization framework that determines both optimal network configurations and protective device settings for multiple PV generation scenarios.

From the above review, it is evident that:

- Conventional DNR is generally protection-blind.
- Protection-aware DNR often relies on fixed relay settings.
- Relay re-coordination methods have not been sufficiently extended to DG-integrated feeders.

Therefore, a gap exists in combining DG-aware reconfiguration with non-adaptive relay re-coordination in a unified and practical framework. This paper addresses this gap by proposing a co-optimization approach that integrates these aspects in a concise and implementable form.

The contribution of this paper is not the introduction of a new optimization algorithm or a new protection principle. Rather, the work extends the previously developed non-adaptive reconfiguration and relay re-coordination framework to a PV-integrated distribution network under combined load and PV operating uncertainty. In contrast to studies that consider distributed generation and protection constraints with fixed protective settings, the proposed formulation determines network configurations together with one universal set of overcurrent-relay TMS values that remains unchanged across all selected operating scenarios.

The main contributions of this paper are therefore summarized as follows:

1. Extension of the offline non-adaptive relay re-coordination framework to PV-integrated distribution networks under multiple load and PV operating scenarios.
2. Joint enforcement of a single universal relay TMS set across all selected network configurations and operating scenarios, while allowing the network topology to change according to the operating condition.
3. Quantitative comparison with fixed-setting and adaptive-protection approaches in terms of network losses, feasible configurations, relay operating time, and coordination margin.
4. A practical offline implementation structure in which the relay settings are calculated once, while only pre-approved network switching actions are applied during operation.

The remainder of this paper is organized as follows: Section 2 reviews relevant literature. Section 3 formulates the optimization problem. Section 4 details the proposed methodology. Section 5 presents simulation results, and Section 6 concludes the paper.

2. Problem Formulation

2.1. Objective Functions & Constraints

The proposed method aims to simultaneously minimize total active power loss and maximize protection coordination flexibility across multiple network configurations under varying PV generation and load conditions. The multi-objective optimization problem and its constraints are formulated as follows. Power loss minimization is written in (1), and constraints are formulated for Power Flow Equations, Voltage Limits, Line Thermal Limits, PV Generation Limits, and the Radiality Constraint in (2) to (7).

The main objective is defined as the minimization of total active power loss in the reconfigured DG-integrated feeder:

$$\min P_{\text{loss}} = \sum_{(i,j)\in\Omega_{br}} R_{ij} \; |I_{ij}|^2 \tag{1}$$

where Ω_{br} is the set of energized branches.

$$P_{i,c} = V_{i,c} \sum_{k=1}^{N_{bus}} V_{k,c} \left(G_{ik} \cos \theta_{ik,c} + B_{ik} \sin \theta_{ik,c}\right) \quad (2)$$

$$Q_{i,c} = V_{i,c} \sum_{k=1}^{N_{bus}} V_{k,c} \left(G_{ik} \sin \theta_{ik,c} - B_{ik} \cos \theta_{ik,c}\right) \quad (3)$$

$$V^{\min} \leq V_{i,c} \leq V^{\max} \quad (4)$$

$$0 \leq P_{PV,i,c} \leq P_{PV,i}^{\max} \quad (5)$$

$$Q_{PV,i,c} = P_{PV,i,c} \cdot \tan\left(\cos^{-1}(pf_{PV})\right) \quad (6)$$

$$N_{br} = N_{bus} - N_{sub} \quad (7)$$

where N_{sub} is the number of substations.

The post-reconfiguration topology must remain radial and connected. In this paper, radiality is enforced through a fundamental-loop-based encoding in the outer optimization process, so that exactly one branch from each fundamental loop is opened and no isolated node is created. This implementation follows the conventional reconfiguration logic used in prior protective-constraint studies.

Protection coordination constraints are shown in (8) to (15). The pickup current of each relay must be selected above the maximum load current flowing through that relay, considering an overload factor:

$$I_{p,r} \geq OF \times I_{load,r}, \forall r \quad (8)$$

where OF is the overload factor. A normal inverse overcurrent characteristic is adopted. Therefore, the operating time of relay $r$is given by:

$$t_r = \frac{0.14\, TMS_r}{\left(\frac{I_{f,r}}{I_{p,r}}\right)^{0.02} - 1} \forall r \quad (9)$$

This structure is consistent with both the protective-constraint benchmark and the authors' previous relay re-coordination work. For each main-backup relay pair, the operation time of the backup relay must exceed that of the main relay by at least the minimum coordination interval:

$$t_b - t_m \geq CTI_{\min} \quad (10)$$

In this paper, the minimum coordination interval is taken as:

$$CTI_{\min} = 0.30 \text{ s} \quad (11)$$

which is consistent with the previous benchmark studies. In this study, the term non-adaptive means that the overcurrent relay settings are determined once in the offline optimization stage and remain unchanged during network operation. The network topology may vary among the preselected operating scenarios, but the relay Time Multiplier Settings (TMS) are not recalculated or updated online after each switching action. Therefore, a single universal TMS value is assigned to each relay and must satisfy all primary–backup coordination constraints for every selected network configuration and operating scenario considered in the optimization. Since the protection philosophy of this paper is non-adaptive, one fixed set of relay settings must remain valid for all studied configurations or operating conditions:

$$\begin{aligned} TMS_{r,s} &= TMS_r, \forall r, \forall s \\ TMS_{r.c.s} &= TMS_r^* \qquad \forall r.c.s \end{aligned} \quad (12)$$

where s denotes the operating scenario. $TMSr*$ denotes the unique offline setting of relay r, which is common to all selected configurations c and operating scenarios s.

Once a candidate network configuration is generated, the relay settings are obtained by solving the following subproblem:

$$\min \frac{1}{N_s} \sum_{s=1}^{N_s} \left(\frac{1}{N_r} \sum_{r=1}^{N_r} t_{r,s} \right) \quad (13)$$

$$TMS_r^{\min} \leq TMS_r \leq TMS_r^{\max} \quad (14)$$

$$t_{b,s} - t_{m,s} \geq CTI_{\min}, \forall (m,b), \forall s \quad (15)$$

Thus, the outer problem minimizes network loss, while the inner relay-setting problem guarantees secure coordination with minimum average operating time. This ensures a single set of relay settings is used for all configurations.

2.2. PV Uncertainty Modeling

PV output power is modeled using the Beta distribution for solar irradiance:

$$f(G) = \frac{\Gamma(\alpha+\beta)}{\Gamma(\alpha)\Gamma(\beta)} \left(\frac{G}{G_{\max}}\right)^{\alpha-1} \left(1 - \frac{G}{G_{\max}}\right)^{\beta-1} \quad (16)$$

where G is solar irradiance, $G_{\max}$ is maximum irradiance, and α, β are shape parameters. The PV output power is then:

$$P_{PV} = P_{rated} \cdot \frac{G}{G_{std}} \cdot \eta \quad (17)$$

where η is efficiency and $G_{std} = 1000\, W/m^2$. A scenario-based approach is used to model uncertainties in load and PV generation:

$$S = \{(P_{load,s}, Q_{load,s}, P_{PV,s})\}, s = 1, \dots, N_s \quad (18)$$

where each scenario s represents a possible realization of uncertain parameters.

3. Method

3.1. Integrated GA-LP Framework for PV-Integrated Network Reconfiguration

The proposed methodology integrates a Genetic Algorithm (GA) for distribution network reconfiguration with Linear Programming (LP) for offline overcurrent relay re-coordination, explicitly incorporating PV generation uncertainty. The framework is designed to determine a single set of relay settings (TMS) that remain valid across multiple optimal network configurations under varying PV output and load conditions, without requiring real-time telecommunication infrastructure.

3.2. Overall Algorithm Flowchart

The step-by-step procedure is described as follows:

Step 1: Input Data & Scenario Generation

- Network topology, line parameters, protective device locations, PV installation sites.
- Historical/PV generation profiles (Beta distribution) and load profiles (Normal distribution).
- Generate N_s scenarios for PV/load uncertainty using the scenario-based method from [2].

Step 2: GA Initialization

- Population size = 50, crossover rate = 0.6, mutation rate = 0.01.
- Chromosome encoding: each gene represents an open switch per fundamental loop (ensures radiality).

Step 3: Fitness Evaluation (Per Candidate Configuration)

- Run power flow for each scenario to compute P_{loss} and voltage profile.
- Solve LP sub-problem for relay coordination:
  - Pickup currents (I_p) fixed based on max load current across all scenarios.
  - LP optimizes TMS to minimize relay operating times while satisfying CTI ≥ 0.3 s.
  - Constraint: $TMS_{r,c1} = TMS_{r,c2}\ \forall$ configurations $c1, c2$.

Step 4: Multi-Objective Fitness Function

$$Fitness = w_1 \frac{P_{loss}}{P_{loss,base}} + w_2 \frac{\max(t_{relay})}{t_{base}} + \sum Penalties \quad (19)$$

Penalties for: voltage violations, line overloads, protection miscoordination.

Step 5: Genetic Operators

- Selection: Tournament selection.
- Crossover: Single-point crossover (preserves radiality via fundamental loops).
- Mutation: Random switch change within the same loop.

Step 6: Termination & Output

- Stop after 100 generations or convergence.

Output: Pareto-optimal set of configurations + universal TMS settings for all relays

3.3. Protection Coordination LP Formulation

For each configuration c and scenario s, the LP model is:

$$\min \sum_{r=1}^{N_r} TMS_r \quad (20)$$

$$TMS^{\min} \le TMS_r \le TMS^{\max} \quad (21)$$

$$t_{b,r,c,s} - t_{m,r,c,s} \ge 0.3 \forall \text{ P/B pairs} \quad (22)$$

$$t_{r,c,s} = TMS_r \cdot \frac{0.14}{(PSM_{r,c,s})^{0.02} - 1} \quad (23)$$

$$PSM_{r,c,s} = \frac{I_{fault,r,c,s}}{I_{p,r}} \quad (24)$$

$$TMS_{r,c1} = TMS_{r,c2} \forall c1, c2 \quad (25)$$

3.4. PV Uncertainty Modeling via Strategy

1. Generate 1000+ scenarios of PV output using a Beta distribution for irradiance.
2. Apply the **backward reduction algorithm** to select 12 representative scenarios.
3. Each scenario includes:
   - PV output at each PV bus.
   - Corresponding load level (residential/commercial/industrial).

The practical implementation strategy is proposed as follows:

- **Offline computation**: Yearly schedule of configurations per scenario.
- **Field operation**: Operator switches the network to a pre-computed configuration based on time/season.

No real-time communication: Relays keep fixed TMS settings optimized offline

4. Result and Discussion

4.1. Test Systems and Simulation Setup

The proposed method is tested on two distribution networks: the IEEE 33-bus system and the Sirjan 78-bus system. The IEEE system includes 33 buses, 32 branches, five tie-switches, and a nominal voltage of 12.66 kV. The Sirjan system includes 78 buses, 77 branches, five tie-switches, and a nominal voltage of 20 kV.

PV units are installed at predetermined buses based on optimal DG allocation studies. For the IEEE 33-bus system, three PV units of 300 kW are located at buses 6, 15, and 31. For the Sirjan 78-bus system, five PV units are located at buses 12, 25, 41, 55, and 70, with rated capacities of 200, 250, 300, 250, and 200 kW, respectively. The PV installation specifications of both test systems are listed in Table 6. Overcurrent relays are placed at substations and feeder heads according to the coordination principles described in Section 3.

Uncertainty is represented by 12 scenarios, obtained from three load levels and four PV output levels. Load uncertainty is modeled using normal distributions, while solar irradiance is modeled using Beta distributions. All simulations are performed in MATLAB 2021b on a PC with an Intel Core i7-10750H processor and 16 GB RAM.

From an implementation viewpoint, the proposed offline optimization provides a predefined operating schedule. For each representative scenario, the network topology is selected in advance, while a single fixed set of relays TMS values is kept unchanged. Therefore, field operation only requires switching to the precomputed configuration, without online relay resetting or real-time communication.

Load-flow analysis is performed in a single-phase framework and generalized to the three-phase system. Short-circuit calculations show that the three-phase fault level at the substation remains between 60 and 80 MVA in all test cases. Three-phase bolted faults are considered because they generally produce the highest fault currents and provide a conservative basis for relay coordination. Load current is neglected during fault conditions.

Daily load patterns for working days and weekends in different seasons are represented by three 8-hour intervals. The maximum active and reactive demands, load categories, and load shares at each bus are adopted from [17]. The PV locations, capacities, and generation profiles are adopted from [22].

4.2. Load Demand and PV Data

Fig. 1 shows the normal distribution of active load demand for the IEEE 33-bus system. Three load levels are considered: low load of 2229 kW, corresponding to 0.6 p.u.; medium load of 2972 kW, corresponding to 0.8 p.u.; and high load of 3715 kW, corresponding to 1.0 p.u. The probabilities of these levels are 0.25, 0.50, and 0.25, respectively. For each level, the standard deviation is assumed to be 10% of the mean value.

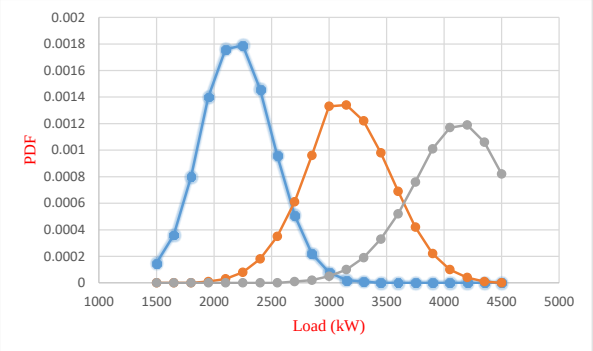


Fig. 1. Probability density function of load demand (IEEE 33-bus system)

Fig. 2 shows the Beta probability density functions used for solar irradiance. Four PV output levels are considered: very low irradiance of 50 W/m², low irradiance of 250 W/m², medium irradiance of 500 W/m², and high irradiance of 900 W/m². The corresponding Beta shape parameters are selected as (2, 4), (3, 3), (4, 2), and (5, 1.5), respectively. The probabilities of the four PV levels are 0.2, 0.3, 0.3, and 0.2.

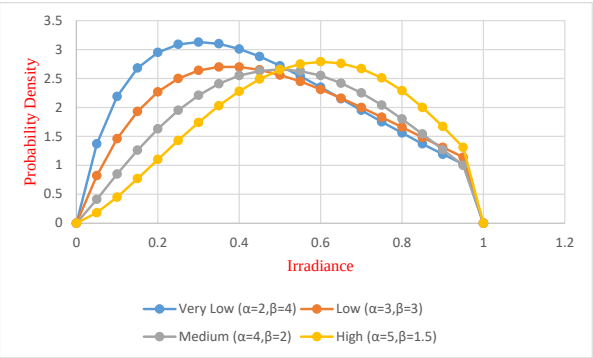


Fig. 2. Beta distribution of solar irradiance for four PV generation levels

Fig. 3 presents the hourly irradiance profiles for four representative day types: summer weekday, summer weekend, winter weekday, and winter weekend. Summer profiles have higher peak irradiance, approximately 900 W/m², and longer daylight duration, while winter profiles have lower peak irradiance, approximately 500 W/m², and shorter daylight duration. Combining the three load levels with the four PV levels gives the 12 scenarios used in the optimization framework.

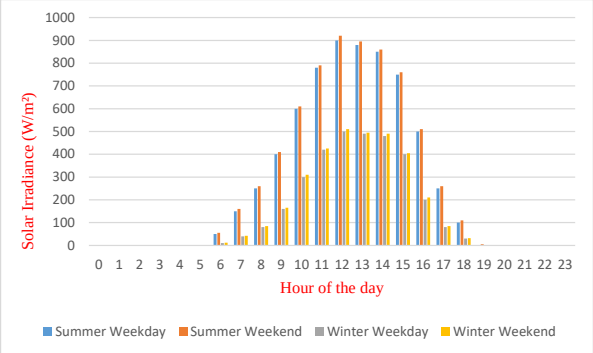


Fig. 3. Daily solar irradiance profiles for four representative day types

4.3. IEEE 33-bus System

To further clarify the effectiveness of the proposed method, three protection strategies are compared under the same reconfiguration framework: adaptive protection, fixed protection settings, and offline non-adaptive re-coordination. The adaptive approach provides the largest feasible search space because relay settings can be updated after each topology change, but this requires online setting changes and communication support. The fixed-setting approach avoids online adaptation but restricts the number of admissible configurations because the original relay settings must remain coordinated after reconfiguration. The proposed method occupies an intermediate position: relay settings remain fixed during operation, as in the non-adaptive case, but they are re-coordinated offline over the selected set of configurations. Consequently, the feasible configuration space is substantially enlarged compared with the fixed-setting approach, while the resulting loss remains close to the adaptive benchmark.

For the IEEE 33-bus system, the proposed method is evaluated under both without-PV and with-PV conditions. The without-PV case is used to compare the results with the previous study in [17], while the with-PV case is used to quantify the effect of PV integration on loss reduction and protection coordination.

The comparison with the closest published studies also clarifies the methodological position of the present work. Reference [17] demonstrated that offline relay re-coordination can significantly recover low-loss configurations in reconfigurable networks, but distributed generation was not considered. Reference [21] incorporated DG, protection constraints, and uncertainty into the reconfiguration problem, but the protective settings were not jointly re-coordinated as optimization variables. The present study extends the former approach to PV-integrated operation while retaining one universal relay-setting set across the considered operating scenarios.

Table (2): Performance comparison of protection strategies for the IEEE 33-bus system with and without PV

Method	Aggregated Loss over 12 Operating States (kW)	No. of Feasible Configs	Min CTI (s)	Avg. Relay Time (s)
Initial Configuration (no PV)	2801.5	1	>0.30	1.45
Initial Configuration (with PV)	1563.24	1	>0.30	1.52
Reconfig. Adaptive protection method (no PV)	1684.5	١٢	>0.35	0.92
Reconfig. Adaptive protection method (with PV)	639.95	12	>0.30	0.95
Reconfig. with fixed protection settings (no PV)	2472.37	3	>0.20	1.20
Reconfig. with fixed protection settings (with PV)	1479.6	2	>0.20	1.18
Reconfig. with re-coordination (no PV)	1684.٨	9	>0.30	0.96
Proposed method – Loss minimization	648.2	11	>0.30	0.98
Proposed method – Time minimization	1120.5	8	>0.30	0.68

As shown in Table 2, the reported value of 2801.5 kW for the initial configuration without PV is not the power loss of a single operating point of the standard IEEE 33-bus system. It is the

aggregated loss objective obtained by summing the active-power losses over the 12 representative operating states considered in the study. Therefore, this value should not be directly compared with the conventional single-state base-case loss values commonly reported for the IEEE 33-bus benchmark.

Therefore, the effectiveness of the proposed method should be interpreted as a compromise between the operational flexibility of adaptive protection and the implementation simplicity of fixed-setting protection.

After installing three PV units of 300 kW at buses 6, 15, and 31, the loss decreases to 1563.24 kW, corresponding to a 44.2% reduction. This reduction is caused by local active power injection, which reduces current flow in the main feeder sections. The minimum CTI remains higher than 0.30 s, while the average relay operating time increases from 1.45 s to 1.52 s because inverter-based PV reduces the effective fault current seen by some relays.

The adaptive protection method gives the best reference performance because relay settings are updated after each reconfiguration. Without PV, it reduces the loss from 2801.5 kW to 1684.5 kW, corresponding to a 39.9% reduction. It also provides 12 feasible configurations, CTI above 0.35 s, and an average relay operating time of 0.92 s. With PV, the loss further decreases to 639.95 kW, which is 59.0% lower than the initial configuration with PV. The CTI remains above 0.30 s, and the average relay operating time is 0.95 s. However, this method requires reliable telecommunication infrastructure and online setting adjustment.

The fixed protection setting method is much more restrictive. Without PV, it reduces the loss only to 2472.37 kW, corresponding to an 11.8% reduction compared with the initial configuration. Only 3 feasible configurations are obtained, and the minimum CTI is 0.20 s, which is below the required 0.30 s margin. With PV, the loss decreases to 1479.6 kW, which is only 5.4% lower than the initial configuration with PV. The number of feasible configurations drops to 2, and the minimum CTI remains 0.20 s. These results show that fixed settings severely limit the feasible search space, especially when PV is present.

The offline re-coordination method without PV achieves a loss of 1684.8 kW, which is almost the same as the adaptive method without PV. It provides 9 feasible configurations, maintains CTI above 0.30 s, and gives an average relay operating time of 0.96 s. This confirms that offline re-coordination can recover most of the benefit of adaptive protection without requiring online communication.

With PV, the proposed loss-minimization method achieves a loss of 648.2 kW. This is 58.5% lower than the initial configuration with PV and only 1.3% higher than the adaptive protection results of 639.95 kW. The number of feasible configurations increases to 11, compared with only 2 in the fixed-setting method, while CTI remains above 0.30 s. The average relay operating time is 0.98 s, which is slightly higher than the adaptive case because of the PV-induced reduction in fault current.

These results indicate that the main benefit of the proposed method is not only the reduction of active-power loss, but also the recovery of network configurations that would otherwise be excluded by fixed relay settings. The increase in the number of feasible configurations from 2 to 11 shows that offline relay re-coordination relaxes the protection-induced restriction on the reconfiguration search space. At the same time, the minimum CTI remains above the required 0.30 s, indicating that the additional operational flexibility is obtained without sacrificing relay selectivity. The small difference between the proposed and adaptive-protection loss values also suggests that most of the operational benefit of adaptive protection can be retained without online relay-setting changes.

When the objective is changed to relay-time minimization, the maximum relay operating time decreases from 0.98 s to 0.68 s, corresponding to a 30.6% improvement. This improvement is obtained at the cost of increasing the loss from 648.2 kW to 1120.5 kW, which is a 72.8% increase. The number of feasible configurations also decreases from 11 to 8 because some low-time configurations cannot satisfy the required CTI margin.

The PV penetration study, summarized in Table 3, confirms the same trend. At 0% PV penetration, the proposed method gives a loss of 1684.5 kW and a maximum relay time of 0.96 s. As PV penetration increases to 25%, 50%, 75%, and 100%, the losses decrease to 1250.0, 950.0, 780.0, and 648.2 kW, respectively. Over the same range, the maximum relay time slightly increases from 0.96 s to 0.98 s, while CTI remains above 0.30 s in all cases.

Fig. 4 presents the Pareto front for the IEEE 33-bus system with PV integration. The loss-minimizing point is 648.2 kW with a relay operating time of 0.98 s, while the time-minimizing

point is 1120.5 kW with a relay operating time of 0.68 s. The intermediate non-dominated solutions show the trade-off between energy efficiency and relay operating speed.

Table (3): Effect of PV penetration level on the proposed method for the IEEE 33-bus system

PV Penetration (%)	Total PV (kW)	Total Loss (kW)	Max Relay Time (s)	Min CTI (s)
0	0	1684.5	0.96	>0.30
25	225	1250.0	0.97	>0.30
50	450	950.0	0.975	>0.30
75	675	780.0	0.98	>0.30
100	900	648.2	0.98	>0.30

We assume that the PV is installed gradually from 0% to 100% of the rated capacity (0 to 900 kW) and the proposed method (re-coordination) is applied. The following numbers are consistent with the previous results (at 100%-point losses = 648.2 and relay time = 0.98).

Figure 4 presents the Pareto front for the IEEE 33-bus system with PV integration, illustrating the trade-off between active power loss minimization and relay operating time minimization. Point A (648.2 kW, 0.98 s) corresponds to the configuration with minimum losses, while Point J (1120.5 kW, 0.68 s) corresponds to the configuration with minimum relay operating time. The intermediate points represent non-dominated solutions where neither objective can be improved without degrading the other. The Pareto front exhibits a convex shape, with a steeper slope in the region near Point A, indicating that small increases in losses initially yield significant improvements in relay speed. However, beyond the mid-region, further reductions in relay time require disproportionately large increases in losses.

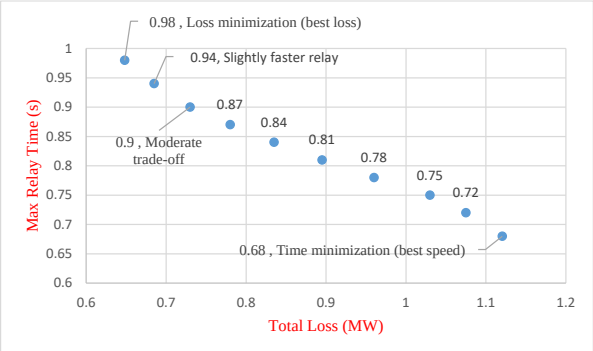


Fig. 4. Pareto front for IEEE 33-Bus system (with PV)

The Pareto results also show that loss minimization and relay-speed minimization are conflicting objectives. Faster relay operation requires larger TMS adjustments and leads the optimization toward configurations with higher network losses. Therefore, the Pareto front provides an operational trade-off rather than a single universally optimal solution. In practice, the loss-oriented solution is more suitable for normal operation, whereas a faster relay-response solution may be preferred when protection speed is given higher priority.

4.4. Sirjan 78-Bus System

The Sirjan 78-bus distribution system is used to evaluate the scalability of the proposed framework. This system includes 78 buses, 77 branches, five tie-switches, and six overcurrent relays. The base power is 100 MVA and the nominal voltage is 20 kV.

In the initial configuration without PV, the total loss is 6556 kW. After installing PV units with a total capacity of 1200 kW, the loss decreases to 3820 kW, corresponding to a 41.7% reduction. The average relay operating time increases from 1.65 s to 1.72 s because PV integration reduces the fault current contribution seen by some relays. The minimum CTI is 0.25 s without PV, which indicates partial violation of the standard 0.30 s margin. With PV, the minimum CTI improves to 0.30 s.

For the adaptive protection method, the loss decreases from 6556 kW to 4112 kW without PV, corresponding to a 37.3% reduction. All 16 candidate configurations are feasible; the CTI exceeds 0.40 s, and the average relay operating time is 1.05 s. With PV, the adaptive method reduces the loss to 1650 kW, corresponding to a 56.8% reduction compared with the initial configuration with PV. The CTI remains above 0.35 s, and the average relay operating time is 1.08 s. This case represents the ideal benchmark, but it requires online communication and setting updates.

The fixed protection setting method again shows limited performance. Without PV, the loss is reduced to 5227.7 kW, which is only a 20.3% reduction compared with the initial configuration. Only 4 out of 16 configurations are feasible, and the minimum CTI is 0.25 s. With PV, the loss decreases to 3100 kW, corresponding to an 18.8% reduction compared with the initial configuration with PV. The number of feasible configurations decreases to 3, the CTI remains 0.25 s, and the average relay operating time increases to 1.38 s.

The proposed method without PV reduces the loss to 4220.3 kW, corresponding to a 35.6%

reduction compared with the initial configuration. It provides 13 feasible configurations out of 16, maintains CTI above 0.35 s, and gives an average relay operating time of 1.15 s. Therefore, it approaches the adaptive protection result while avoiding communication infrastructure.

With PV, the proposed method reduces the loss to 1680 kW. This is 56% lower than the initial configuration with PV and only 1.8% higher than the adaptive protection result of 1650 kW. The number of feasible configurations increases to 14, compared with only 3 in the fixed-setting method. The CTI remains above 0.35 s, and the average relay operating time is 1.18 s.

The Sirjan results confirm that the same behavior is preserved in a larger and more practical network. The proposed method substantially increases the number of protection-feasible configurations compared with the fixed-setting case, while its loss performance remains close to the adaptive benchmark. This indicates that the advantage of offline re-coordination is not limited to the IEEE 33-bus test system and can remain effective as the network size and number of protection constraints increase.

The time-minimization case shows the same trade-off observed in the 33-bus system. Reducing the maximum relay operating time from 1.18 s to 0.82 s gives a 30.5% improvement in relay speed, but the loss increases from 1680 kW to 2850 kW, corresponding to a 69.6% increase. The number of feasible configurations also decreases from 14 to 10.

The PV penetration study for the Sirjan 78-bus system, summarized in Table 4, shows that increasing PV capacity reduces network losses while slightly increasing relay operating time. At 0% PV penetration, the loss is 4220.3 kW and the maximum relay time is 1.15 s. At 25%, 50%, 75%, and 100% PV penetration, the losses decrease to 3100.0, 2450.0, 2000.0, and 1680.0 kW, respectively. The maximum relay time increases only from 1.15 s to 1.18 s, and CTI remains above 0.35 s in all cases.

Fig. 5 presents the Pareto front for the Sirjan 78-bus system with PV integration. The loss-minimizing point is 1680 kW with a relay operating time of 1.18 s, while the time-minimizing point is 2850 kW with a relay operating time of 0.82 s. These results confirm that the proposed method remains effective for a larger network and provides a practical compromise between loss reduction and protection speed.

Table (4): Effect of PV penetration level on the proposed method for the Sirjan 78-bus system

PV Penetration (%)	Total PV (kW)	Total Loss (kW)	Max Relay Time (s)	Min CTI (s)
0	0	4220.3	1.15	>0.35
25	300	3100.0	1.16	>0.35
50	600	2450.0	1.17	>0.35
75	900	2000.0	1.175	>0.35
100	1200	1680.0	1.18	>0.35

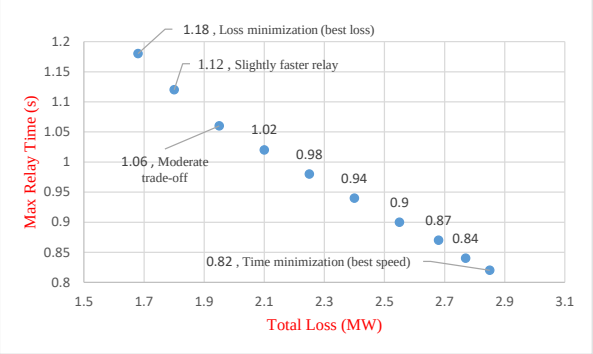


Fig. 5. Pareto front for Sirjan 78-Bus system (with PV)

Table (5): Comparison of two objectives for the proposed method

Network	Objective	Loss (kW)	Max Relay Time (s)	No. of Feasible Configs
33-bus	Loss minimization	648.2	0.98	11
33-bus	Time minimization	1120.5	**0.68**	8
78-bus	Loss minimization	1680	1.18	14
78-bus	Time minimization	2850	**0.82**	10

Table 5 compares the two objective functions considered in the proposed method. For the IEEE 33-bus system, loss minimization gives 648.2 kW and 0.98 s, while time minimization gives 1120.5 kW and 0.68 s. For the Sirjan 78-bus system, loss minimization gives 1680 kW and 1.18 s, while time minimization gives 2850 kW and 0.82 s. In both systems, faster relay operation is obtained only by accepting higher active power losses and fewer feasible configurations. This confirms the inherent trade-off between energy efficiency and protection speed.

4.5. Scalability and Computational Efficiency

The GA-LP framework shows acceptable scalability when moving from the IEEE 33-bus system to the Sirjan 78-bus system. The computational burden increases with system size

because more branches, candidate configurations, and relay coordination constraints must be evaluated. However, the increase remains suitable for offline planning.

Scenario reduction also has a significant effect on computation time. Reducing more than 1000 initial uncertainty scenarios to 12 representative scenarios decreases the computational time by about 65% compared with full Monte Carlo simulation. Therefore, the proposed method can generate an annual operating schedule without requiring real-time optimization.

4.6. Analysis of Protection Coordination Under PV Variability

PV integration reduces branch currents during normal operation, but it can also reduce the fault current seen by overcurrent relays. This may increase relay operating time and may lead to loss of coordination if relay settings are kept fixed.

The proposed method compensates for this effect by optimizing a universal set of TMS values over all selected configurations and uncertainty scenarios. In the IEEE 33-bus system, CTI remains above 0.30 s for all PV penetration levels. In the Sirjan 78-bus system, CTI remains above 0.35 s. Therefore, the proposed non-adaptive setting strategy preserves protection selectivity under PV variability without online relay resetting.

Table (6): PV installation specifications

System	PV Bus Location	Rated Capacity (kW)	Number of Units	Total PV Capacity (kW)
IEEE 33-bus	6, 15, 31	300 each	3	900
Sirjan 78-bus	12, 25, 41, 55, 70	200, 250, 300, 250, 200	5	1200

4.7. Practical Implementation Advantages

In practical implementation, relay re-coordination is performed only during the offline planning stage. First, the expected load and PV operating scenarios and the corresponding candidate network configurations are evaluated. The short-circuit currents and primary–backup relay pairs are then determined for all selected operating states. Using these data, the LP-based coordination problem is solved once to obtain a single universal set of relay TMS values satisfying the required CTI for all selected configurations and scenarios. These TMS values are subsequently entered into the digital overcurrent relays and remain unchanged during normal operation.

During operation, only the network switching configuration may change according to the precomputed operating schedule or the identified load/PV condition. No online recalculation or downloading of relay settings is required after each reconfiguration. Therefore, the proposed scheme does not eliminate the possible use of SCADA or remote switching for network operation; rather, it eliminates the need for real-time communication specifically for adaptive relay-setting updates.

Compared with adaptive protection schemes, the proposed method does not require real-time communication for adaptive relay-setting updates or real-time relay setting changes. The relay settings are calculated offline and remain fixed during operation. The operator only applies the precomputed switching configuration corresponding to the expected load and PV scenario.

This structure is compatible with existing digital relays and can also be applied in systems where communication-based adaptive protection is not economically justified. The offline schedule can account for seasonal load variation, day type, and PV generation level while maintaining the required protection coordination margin.

Accordingly, practical deployment requires three offline steps: scenario and configuration assessment, short-circuit and coordination analysis, and installation of the resulting universal TMS values in the relays. During subsequent operation, the operator applies only pre-approved switching configurations while the relay settings remain fixed.

4.8. Computational Time Comparison

Table 7 compares the computational time of the proposed method with conventional uncertainty evaluation techniques. Monte Carlo simulation with 35000 scenarios requires approximately 600 min for the 33-bus system. The two-point estimation method requires 87.6 min, while a scenario-based method with 40 scenarios requires 5.96 min.

The proposed GA-LP method is considerably faster. For the 33-bus system without PV, the simulation time is 0.19 min (11.36 s). With PV and 12 uncertainty scenarios, the time increases to about 0.42 min (25 s). For the Sirjan 78-bus system with PV and 12 scenarios, the simulation time is about 0.75 min (45 s). These results confirm that the proposed method is computationally efficient for offline planning.

Table (7): Computational time comparison

Method	System	Simulation Time (min)
Monte Carlo (35000 scenarios)	33-bus	~600
TPEM (640 runs)	33-bus	87.6
Scenario-based (40 scenarios)	33-bus	5.96
Proposed GA-LP (without PV)	33-bus	0.19 (11.36 sec)
Proposed GA-LP (with PV, 12 scenarios)	**33-bus**	**~0.42 (25 sec)**
Proposed GA-LP (with PV, 12 scenarios)	**78-bus**	**~0.75 (45 sec)**

5. Conclusion

This paper extended an offline non-adaptive overcurrent-relay re-coordination framework to PV-integrated distribution-network reconfiguration under multiple load and PV operating scenarios. The contribution is not a new optimization algorithm or protection principle; rather, it is the joint consideration of PV-integrated reconfiguration and offline relay re-coordination while maintaining one universal set of relay Time Multiplier Settings (TMS) across all selected configurations and operating scenarios.

The results obtained for the IEEE 33-bus and Sirjan 78-bus systems show that fixed protection settings can significantly restrict the feasible reconfiguration space. Offline re-coordination increases the number of protection-feasible configurations and allows lower-loss operating states to be selected while maintaining the required coordination time interval. The proposed approach therefore provides performance close to the adaptive-protection benchmark without requiring online relay-setting updates.

The Pareto analysis also demonstrates the trade-off between active-power loss reduction and relay operating speed. Solutions with faster relay operation generally require accepting higher network losses, allowing the system operator to select an operating point according to the relative importance of efficiency and protection speed.

From a practical perspective, the relay settings are calculated once during the offline planning stage and remain unchanged during operation. Only pre-approved network configurations are selected according to the operating condition. Therefore, the proposed method avoids the need for real-time communication specifically for adaptive relay-setting changes while retaining greater reconfiguration flexibility than conventional fixed-setting protection.

Future work may extend the framework to unbalanced three-phase operation, detailed inverter-based PV fault-current models, and coordination with additional protective devices such as fuses and reclosers.

Nomenclature

Variables & Parameters	Definition
P_{loss}	Total active power loss of the network (kW)
P_i	Active power injected at bus i (kW)
Q_i	Reactive power injected at bus i (kVAr)
V_i	Voltage magnitude at bus i (p.u.)
$V^{\min}.V^{\max}$	Minimum and maximum allowable bus voltage (p.u.)
I_j	Current flowing through branch j (A)
$I_j^{\max}$	Maximum current limit of branch j (A)
R_j	Resistance of branch j (Ω)
t_r	Operating time of relay r (s)
TMS_r	Time Multiplier Setting of relay r (dimensionless)
$TMS^{\min}.TMS^{\max}$	Lower and upper bounds of TMS
$I_{p.r}$	Pickup current of relay r (A)
$I_{fault.r}$	Short-circuit current seen by relay r (A)
PSM	Plug Setting Multiplier (dimensionless)
CTI	Coordination Time Interval (s)
t_{margin}	Coordination time margin (usually 0.3 s)
MCT	Maximum Clearing Time of a fuse (s)
MMT	Minimum Melting Time of a fuse (s)
OLF	Overload Factor (dimensionless)
$P_{PV.i}$	PV output power at bus i (kW)
P_{rated}	Rated power of PV unit (kW)
G	Solar irradiance (W/m²)
G_{std}	Standard irradiance (1000 W/m²)
η	Efficiency of PV panel
α, β	Shape parameters of Beta distribution
N_{br}	Number of branches
N_{bus}	Number of buses
N_r	Number of overcurrent relays
N_s	Number of scenarios
N_{sub}	Number of substations
C	Set of configurations
Indices	
$i.k$	Bus index
j	Branch (line) index
r	Relay index
c	Configuration index

s	Scenario (load/PV) index
b	Backup device index
m	Main device index
Functions & Operators	
$f(G)$	Probability density function of Beta distribution for irradiance
$\Gamma(\cdot)$	Gamma function
$I?$	Correlation coefficient
L_0	Lower triangular matrix from Cholesky decomposition
Abbreviations	
GA	Genetic Algorithm
LP	Linear Programming
DG	Distributed Generation
PV	Photovoltaic
DNR	Distribution Network Reconfiguration
P/B	Primary/Backup
TCC	Time-Current Characteristic

References

[1] P. Ushashree, K. S. Kumar, "Power System Reconfiguration in Distribution System for Loss Minimization Using Optimization Techniques: A Review", Wireless Personal Communications, Vol. 128, No. 3, pp. 1907-1940, 2023. https://doi.org/10.1007/s11277-022-10026-3

[2] M. N. Babu, P. K. Dhal, "Impact of Load Flow and Network Reconfiguration for Unbalanced Distribution Systems", Measurement: Sensors, Vol. 32, Art. No. 101078, 2024. https://doi.org/10.1016/j.measen.2024.101078

[3] H. Lotfi, M. E. Hajiabadi, H. Parsadust, "Power Distribution Network Reconfiguration Techniques: A Thorough Review", Sustainability, Vol. 16, No. 23, Art. No. 10307, 2024. https://doi.org/10.3390/su162310307

[4] G. A. D. Vargas, D. J. Mosquera, E. R. Trujillo, "Optimization of Topological Reconfiguration in Electric Power Systems Using Genetic Algorithm and Nonlinear Programming with Discontinuous Derivatives", Electronics, Vol. 13, No. 3, Art. No. 616, 2024. https://doi.org/10.3390/electronics13030616

[5] A. Saedi, M. S. A. Hanifah, H. H. Ladin, S. H. Yusoff, "Optimal Distribution Network Reconfiguration Using Multi-Objective Cuckoo Search Algorithm", IIUM Engineering Journal, Vol. 23, No. 2, pp. 114-124, 2022. https://doi.org/10.31436/iiumej.v23i2.2190

[6] J. Dias Santos, F. Marques, L. P. Garcés Negrete, G. A. Andrêa Brigatto, J. M. López-Lezama, N. Muñoz-Galeano, "A Novel Solution Method for the Distribution Network Reconfiguration Problem Based on a Search Mechanism Enhancement of the Improved Harmony Search Algorithm", Energies, Vol. 15, No. 6, Art. No. 2083, 2022. https://doi.org/10.3390/en15062083

[7] F. J. Ruiz-Rodríguez, S. Kamel, M. H. Hassan, J. A. Dueñas, "Optimal Reconfiguration of Distribution Systems Considering Reliability: Introducing Long-Term Memory Component AEO Algorithm", Expert Systems with Applications, Vol. 249, Art. No. 123467, 2024. https://doi.org/10.1016/j.eswa.2024.123467

[8] S. Halve, S. Raghuwanshi, D. Sonje, "Radial Distribution System Network Reconfiguration for Reduction in Real Power Loss and Improvement in Voltage Profile, and Reliability", Journal of Operation and Automation in Power Engineering, Vol. 14, No. 2, pp. 78-85, 2026. https://doi.org/10.22098/joape.2024.14549.2113

[9] C. Saravanan, N. Vengadachalam, P. Balakrishnan, T. K. S. Sathyanarayanan, "Enhancing Distribution Network Efficiency with Andean Condor Algorithm-Driven Optimal Placement of Distributed Generation and Network Reconfiguration", Electric Power Components and Systems, Vol. 53, No. 16, pp. 2108-2124, 2025. https://doi.org/10.1080/15325008.2024.2343403

[10] M. Ghotbi Maleki, R. Mohammadi Chabanloo, M. Farrokhifar, "Accurate Coordination Method Based on the Dynamic Model of Overcurrent Relay for Industrial Power Networks Taking Contribution of Induction Motors into Account", IET Generation, Transmission & Distribution, Vol. 14, No. 4, pp. 645-655, 2020. https://doi.org/10.1049/iet-gtd.2019.0325

[11] J. Li, J. Feng, M. Huang, S. Liu, G. Wang, "Optimal Protection Coordination for Directional Overcurrent Relays in Radial Distribution Networks with Inverter-Based Distributed Energy Resources", International Journal of Electrical Power & Energy Systems, Vol. 167, Art. No. 110622, 2025. https://doi.org/10.1016/j.ijepes.2025.110622

[12] M. Ghotbi-Maleki, R. Mohammadi Chabanloo, M. R. Taheri, H. H. Zeineldin, "Coordination of Non-Directional Overcurrent Relays and Fuses in Active Distribution Networks Considering Reverse Short-Circuit Currents of DGs", IET Generation, Transmission & Distribution, Vol. 15, No. 18,

pp. 2539-2553, 2021. https://doi.org/10.1049/gtd2.12197

[13] A. Valenzuela, S. Simani, E. Inga, "Automatic Overcurrent Protection Coordination after Distribution Network Reconfiguration Based on Peer-To-Peer Communication", Energies, Vol. 14, No. 11, Art. No. 3253, 2021. https://doi.org/10.3390/en14113253

[14] A. Barranco-Carlos, C. Orozco-Henao, J. Marín-Quintero, J. Mora-Flórez, A. Herrera-Orozco, "Adaptive Protection for Active Distribution Networks: An Approach Based on Fuses and Relays with Multiple Setting Groups", IEEE Access, Vol. 11, pp. 31075-31091, 2023. https://doi.org/10.1109/ACCESS.2023.3261827

[15] B. Khorshid-Ghazani, H. Seyedi, B. Mohammadi-Ivatloo, K. Zare, S. Shargh, "Reconfiguration of Distribution Networks Considering Coordination of the Protective Devices", IET Generation, Transmission & Distribution, Vol. 11, No. 1, pp. 82-92, 2017. https://doi.org/10.1049/iet-gtd.2016.0539

[16] A. S. Kahnamouei, S. Lotfifard, M. Rostami, "Optimized Distribution Systems Reconfiguration Considering Protection Devices Constraints", IEEE Transactions on Power Delivery, Vol. 40, No. 3, pp. 1267-1278, 2025. https://doi.org/10.1109/TPWRD.2025.3542817

[17] R. Abdollahi, R. Mohammadi Chabanloo, "Optimal Distribution Network Reconfiguration with Non-Adaptive Overcurrent Relay Re-Coordination", Electric Power Systems Research, Vol. 255, Art. No. 112668, 2026. https://doi.org/10.1016/j.epsr.2025.112668

[18] F. Mandrile, F. Stella, E. Carpaneto, R. Bojoi, "Grid Fault Current Injection Using Virtual Synchronous Machines Featuring Active Junction Temperature Limitation of Power Devices", IEEE Journal of Emerging and Selected Topics in Power Electronics, Vol. 10, No. 5, pp. 6243-6251, 2022. https://doi.org/10.1109/JESTPE.2022.3154488

[19] W. M. Hamanah, M. I. Hossain, M. Shafiullah, M. A. Abido, "AC Microgrid Protection Schemes: A Comprehensive Review", IEEE Access, Vol. 11, pp. 76842-76868, 2023. https://doi.org/10.1109/ACCESS.2023.3298306

[20] F. Wang, X. Zhang, J. Zhu, H. Xu, H. Sun, W. Wang, "Adaptive Current Protection Scheme for Distribution Network with Inverter-Interfaced Distributed Generation", Electric Power Systems Research, Vol. 247, Art. No. 111864, 2025. https://doi.org/10.1016/j.epsr.2025.111864

[21] V. Fathi, H. Seyedi, B. Mohammadi-Ivatloo, "Reconfiguration of Distribution Systems in the Presence of Distributed Generation Considering Protective Constraints and Uncertainties", International Transactions on Electrical Energy Systems, Vol. 30, No. 5, Art. No. e12346, 2020. https://doi.org/10.1002/2050-7038.12346

[22] P. Murugesan, P. W. David, P. Murugesan, H. Thangaraj, "A Novel Reconfiguration Technique for Solar PV-Based Microgrid System", Renewable Energy, Vol. 243, Art. No. 122573, 2025. https://doi.org/10.1016/j.renene.2025.122573